Saudi Journal of Biological Sciences 28 (2021) 4137–4146

Contents lists available at ScienceDirect

Saudi Journal of Biological Sciences

journal homepage: www.sciencedirect.com

Original article

# E74-like factor 3 suppresses microRNA-485-5p transcription to trigger growth and metastasis of ovarian cancer cells with the involvement of CLDN4/Wnt/β-catenin axis

Lei Kuang [a], Li'an Li [b,*]

[a] Department of Gynecology, Lianyungang First People's Hospital, Lianyungang 222000, Jiangsu, PR China
[b] Department of Gynecology and Obstetrics, First Medical Center of PLA General Hospital, Beijing 100853, PR China

ARTICLE INFO

*Article history:*
Received 19 February 2021
Revised 22 April 2021
Accepted 22 April 2021
Available online 8 May 2021

*Keywords:*
Ovarian cancer
ELF3
miR-485
CLDN4
Wnt/β-catenin

ABSTRACT

Ovarian cancer (OC) is one of the most prevailing gynecological malignancies with high mortality rate, while E74 like ETS transcription factor 3 (ELF3) is reported to be associated with tumorigenesis. This work aims to analyze the role of ELF3 on the suppression of miR-485-5p transcription in OC. Expression of ELF3 in OC and its correlation with overall survival were predicted on a bioinformation system GEPIA. Then, the level of ELF3 in OC tissues and cells and in normal ones was evaluated. Binding relationships between ELF3 and microRNA (miR)-485-5p, and between miR-485-5p and claudin-4 (CLND4) were predicted through Bioinformatics tools. Altered expression of ELF3, miR-485-5p and CLND4 was introduced alone or jointly to probe their influences on OC cell growth. ELF3 was suggested to be highly expressed in OC, which was linked to poor prognosis in patients. Abundant expression of ELF3 was identified in OC tissues and cell lines as relative to the normal ones. ELF3 inhibition suppressed growth and metastasis of OC cells. ELF3 transcriptionally suppressed miR-485-5p expression to further enhance CLDN4 expression. Overexpression of miR-485-5p led to similar trends as ELF3 inhibition did. Importantly, upregulation of CLDN4 was found to block the roles of ELF3 inhibition in OC cells. In addition, the Wnt/signaling pathway suppressed by miR-485-5p mimic was reactivated following CLDN4 overexpression. This study evidenced that ELF3 suppresses miR-485-5p transcription to enhance CLDN4 expression, leading to Wnt/β-catenin activation and promoting OC cell growth and metastasis. This work may provide new ideas for gene-based therapies for OC.
© 2021 The Authors. Published by Elsevier B.V. on behalf of King Saud University. This is an open access article under the CC BY-NC-ND license (http://creativecommons.org/licenses/by-nc-nd/4.0/).

## 1. Introduction

Ovarian cancer (OC) ranks the second most common cause of death among female reproductive cancers around the world (Lheureux et al., 2019). Conventional therapeutic strategies for OC include surgical resection followed with intermittent administration of chemotherapy drugs such as platinum and taxane (Zahedi et al., 2011). However, the prognosis of OC largely depends on the stages. The overall 5-year survival rate of patients at early stages was over 90% while those at late stages with distant metastasis potential was less than 30% (Alimujiang et al., 2019; Cress et al., 2015). Unfortunately, due to the absence of specific symptoms, OC is said as a silent killer with approximately 70% of patients firstly diagnosed at late stages that are hard to be cured with recurrent relapse and metastasis during the clinical course (Stewart et al., 2019). An early diagnosis is reasonably of primary importance for OC control. In addition to this, identifying novel ideas and developing new options to control the malignant behaviors such as proliferation, epithelial to mesenchymal transition (EMT) and the following metastasis of cancer cells are also urgent issues.

E74 like ETS transcription factor 3 (ELF3, also known as ESE-1) is a member of E-26 transcription family and regulates transcription of an extend array of genes participating in cellular transformation and inflammation (Gajulapalli et al., 2016). Both oncogenic (Wang et al., 2014; Zhao et al., 2018) and tumor suppressing (Gondkar

* Corresponding author at: Department of Gynecology and Obstetrics, First Medical Center of PLA General Hospital, No. 28, Fuxing Road, Haidian District, Beijing 100853, PR China.
*E-mail address:* lilian3069@163.com (L. Li).
Peer review under responsibility of King Saud University.

Production and hosting by Elsevier

https://doi.org/10.1016/j.sjbs.2021.04.093
1319-562X/© 2021 The Authors. Published by Elsevier B.V. on behalf of King Saud University.
This is an open access article under the CC BY-NC-ND license (http://creativecommons.org/licenses/by-nc-nd/4.0/).

et al., 2019) roles of ELF3 have been reported depending on the cancer types. Interestingly, mutation of ELF3 was suggested to be implicated in cervical carcinoma progression (Ojesina et al., 2014), and its association with the tumorigenesis of another gynecologic cancer, breast cancer, has also been concluded (Mesquita et al., 2013). But the function of ELF3 in OC and the mechanisms remain largely unknown. MicroRNAs (miRNAs) are small non-coding RNAs whose dysregulation is correlated with different stages of cancer progression thanks to their function in regulating diverse gene expression post-transcriptionally (Harrandah et al., 2018). The data on the bioinformatics System Jasper (http://jaspar.genereg.net/) suggested that ELF3 can bind to the promoter region of miR-485-5p. This miRNA has been found lower in OC cells than in normal ones, whose upregulation reduced the resistance of cells to cisplatin treatment (Qiao et al., 2020). Whether ELF3 regulates miR-485-5p during OC cell progression aroused our attention. In addition, claudin-4 (CLDN4), a member of the claudin family of tight junction proteins that mainly control paracellular ion flux and cell polarity maintenance, was up-regulated in OC (Honda et al., 2006). Additionally, CLDN4 expression was reported to be negatively linked to the survival of patients with OC (de la Fuente et al., 2018). Taken the discussion above, we speculated that ELF3 is possibly implicated in OC pathogenesis via regulating miR-485-5p and CLDN4 expression.

## 2. Materials and methods

### 2.1. Ethics statement

This study was launched with the approval of the Ethics Committee of our hospitaland performed in compliance with the *Declaration ofHelsinki*. Signed informed consent was received from each eligible participant.

### 2.2. Tissue sample collection

During the period from February 2018 to January 2019, 20 pairs of tumor tissues and the adjacent healthy tissues from OC patients who admitted into our hospital were collected. All enrolled patients were diagnosed through imaging and pathological diagnosis without other malignancies, nor a history of radio or chemotherapy. The collected malignant tissues including adenocarcinoma, mucoid carcinoma, epithelioma and mixed tumors were soaked in liquid nitrogen after surgery and then preserved at −80 °C.

### 2.3. Cell culture and treatment

OC cell lines SKOV3 and OVCAR3 acquired from American Type Culture Collection (ATCC, Manassas, VA, USA) were cultured in Dulbecco's modified Eagle's medium (DMEM, Thermo Fisher Scientific Inc., Waltham, MA, USA). Immortalized human ovarian epithelial cell line SV40 purchased from Applied Biological Materials (ABM) Inc. (Richmond, Canada) were cultivated in Prigrow I medium (ABM). The media were supplemented with 10% fetal bovine serum (FBS) and 1% penicillin/streptomycin (Hyclone Company, Logan, UT, USA) and placed in a 37 °C incubator with 5% $CO_2$.

The short-hairpin (sh) RNA targeting ELF3 (sh-ELF3 1, 2, 3#), miR-485-5p mimic, and lentiviral vector (LV) of CLDN4 (LV-CLDN4) and the corresponding controls used for transfection were acquired from GenePharma Co., Ltd. (Shanghai, China). Lipofectamine™ 2000 (Invitrogen, Thermo Fisher) were used for transfection, and the transfection efficacy was evaluated 48 h later according to expression determined by reverse transcription quantitative polymerase chain reaction (RT-qPCR).

### 2.4. Immunohistochemical staining

The tissue samples were fixed, embedded in paraffin, cut into sections (4-μm thick), and then dewaxed, rehydrated, and soaked in 0.3% $H_2O_2$ to block the activity of endogenous peroxidase. After heat-mediated antigen retrieval in Tris/ethylene diamine tetraacetic acid buffer (pH = 9.0), the sections were blocked with 10% normal goat serum (Boster Biological Technology Co., Ltd., Wuhan, Hubei, China) and then incubated with the primary antibodies to ELF3 (1:250, ab97310, Abcam Inc., Cambridge, MA, USA) and CLDN4 (1:1000, ab6721, Abcam). After that, the sections were incubated with biotinylatedimmunoglobulin G (IgG, 1:1000, ab6721, Abcam). Then, the sections were stained with 3,3′-diaminobenzidine (DAB) and imaged under a microscope (OlympusOptical Co., Ltd., Tokyo, Japan) at a ×400 magnification.

### 2.5. RT-qPCR

Total RNA from tissue samples or cells was extracted using the TRIzol reagent (Invitrogen). A PrimeScript RT Reagent Kit (Takara, Tokyo, Japan) and a miScript cDNA Synthesis Kit (Qiagen, Dusseldorf, Germany) was used for cDNA synthesis from mRNA and miRNA, respectively, as per the kit's protocols. Next, the amplified cDNA was used for real-time qPCR using a SYBR Select Master Mix and an ABI Prism 7000 System (Applied Biosystems, Foster City, CA, USA). The primer sequences are presented in Table 1, and GAPDH and 5S were used as internal controls for mRNAs and miRNA, respectively. Relative gene expression was evaluated using the $2^{-\Delta\Delta Ct}$ method.

### 2.6. Cell proliferation measurement

First, a 3-(4, 5-dimethylthiazol-2-yl)-2, 5-diphenyltetrazolium bromide (MTT) assay kit (C0009, Beyotime, Shanghai, China) was used. Cells after transfection were incubated in 96-well plates at $5 \times 10^3$ cells per well. Each well was loaded with 10 μL MTT solution (5 mg/mL) for 4 h of incubation at 37 °C and then mixed with 100 μL formazan solution for another 4 h. Next, the optical density value at 570 nm was read using a microplate reader (Bio-Rad Laboratories, Hercules, CA, USA).

Colony formation assays were further performed. Cells were seeded in 6-well plates at a density of 300 cells per well with three duplicated wells set. After a 10-d cultivation, the cells were fixed in methanol for 20 min and stained using 0.1% crystal violet, after which the number of cell colony was calculated using the Image J software (National Institutes of Health, Bethesda, Maryland, USA).

**Table 1**
Primer sequences for RT-qPCR.

| Gene | Primer sequence (5′–3′) |
|---|---|
| ELF3 | F:CATGACCTACGAGAAGCTGAGC |
| | R: GACTCTGGAGAACCTCTTCCTC |
| miR-485 | F: AGAGGCTGGCCGTGAT |
| | R: GAACATGTCTGCGTATCTC |
| CLDN4 | F: AGTGCAAGGTGTACGACTCGCT |
| | R: CGCTTTCATCCTCCAGGCAGTT |
| GAPDH | F: GTCTCCTCTGACTTCAACAGCG |
| | R: ACCACCCTGTTGCTGTAGCCAA |
| 5S | F: CTCGCTTCGGCAGCACAT |
| | R: TTTGCGTGTCATCCTTGCG |

Note: RT-qPCR, reverse transcription-quantitative polymerase chain reaction; ELF3, ETS transcription factor 3; CLDN4, claudin-4; GAPDH, glyceraldehyde-3-phosphate dehydrogenase.

### 2.7. Cell apoptosis detection

An Annexin V-fluorescein isothiocyanate (FITC)/propidium iodide (PI) kit (Bestbio Biotechnology Co., Ltd., Shanghai, China) was used for cell apoptosis measurement. Cells after transfection were harvested, trypsinized, washed in cold phosphate-buffered saline (PBS), and then resuspended in 1 × Annexin binding buffer till a $1 \times 10^5$ concentration. Next, 100 μL cell suspension was treated with 5 μL Annexin V-FITC and 5 μL PI, respectively, and incubated avoiding light exposure for 15 min. After warm incubation, 400 μL 1× binding buffer was further added, and the apoptosis was determined using a Cell-Quest Software (BD Biosciences, San Jose, CA, USA) and a flow cytometer (FACSCalibur, BD).

Hoechst 33258 staining was further performed. In brief, 48 h after transfection, cell slides were prepared and fixed in 4% paraformaldehyde, and then stained with Hoechst 33,258 solution (HY-15623, MedChemExpress, Monmouth Junction, NJ, USA) avoiding light exposure for 30 min. Thereafter, the images were captured under a fluorescence microscope (Nikon Instruments Inc., Tokyo, Japan) with 5 random fields selected. The apoptosis rate of cells was measured as follows: apoptosis rate (%) = apoptotic cells/total cells × 100%.

### 2.8. Cell migration and invasion assays

A scratch test was performed to evaluate the migrative ability of cells. Cells after transfection were seeded onto 6-well plates at $5 \times 10^5$ cells per well. A pipette tip (200 μL) was used to produce a straight scratch on cells, and the scratch was cleaned by DMEM to remove the scratched cells. Then, the cells were incubated with 0.5% FBS-supplemented DMEM for 24 h. The scratch width at 0 h and 24 h was photographed under an inverted microscope (Olympus). The size of defined blank area was measured using the Image J software, and the migration rate was determined according to the width at 0 h and 24 h.

Cell invasion was evaluated by the Transwell assay. In brief, each apical chamber was pre-coated with 50 μL Matrigel and then filled with 150 μL cell suspension in serum-free DMEM ($2 \times 10^4$ cells per chamber), while each basolateral chamber was loaded with 750 μL 10% FBS-DMEM. After a 24-h warm incubation, the invaded cells were stained with crystal violet and observed under the inverted microscope.

### 2.9. Enzyme-linked immunosorbent assay (ELISA)

Protein levels of apoptosis-related factors B-cell lymphoma-2 (Bcl-2) and Bcl-2-associated X (Bax) were determined using the ELISA kits (Bax: ab199080, Bcl-2, ab119506, Abcam) as per the manufacturer's instructions. Relative expression of the cytokines was determined using the colorimetry.

### 2.10. Chromatin immunoprecipitation (ChIP) assay

A ChIP analysis concerning the promoter of miR-485-5p was determined using an EZ-Magna ChIP assay kit (EMD Millipore, Billerica, MA, USA). In short, SKOV3 and OVCAR3 cells were respectively cross-linked in 1% methanol solution at room temperature and then quenched by glycocoll. The DNA fragments were obtained by ultrasound treatment and treated with antibodies against ELF3 or IgG. The chromatin DNA in the immunoprecipitated compound was analyzed by RT-qPCR.

### 2.11. Western blot analysis

Total protein from OC cells was collected using cell lysis buffer (Beyotime Biotechnology Co., Ltd., Shanghai, China). The protein concentration was examined using a bicinchoninic acid kit (Thermo Fisher Scientific). Next, an equal volume of protein sample (30 μg) was separated on SDS-PAGEand loaded on polyvinylidene fluoride membranes (Millipore). Then, the membranes were blocked with 5% skimmed milk for 1 h and incubated co-cultured with the primary antibodies against E-cadherin (1:1000, #3195, Cell Signaling Technology, Beverly, MA, USA), vimentin (1:1000, #5741, CST), Wnt1 (1:1000, #MA5-15544, Thermo Fisher), β-catenin (1:1000, #13–8400, Thermo Fisher) and GAPDH (1:10000, ab181602, Abcam) at 4 °C overnight, and then with the secondary antibody goat anti-rabbit IgG H&L (HRP) (1:10000, ab97051, Abcam) or goat anti-rabbit IgG H&L (HRP) (1:10000, ab205719, Abcam) at 37 °C for 45 min. The signals of protein band were measured using the enhanced chemiluminescence system (Thermo Fisher Scientific) and developed.

### 2.12. Dual-luciferase reporter gene assay

Binding sites between miR-485-5p and CLDN4 were first predict on StarBase (http://starbase.sysu.edu.cn/). Then, the putative binding sequence was amplified and cloned to pGL3 luciferase reporter vectors (Promega, Madison, WI, USA) to construct pGL3-based wide type (WT) vector pGL3-CLDN4-WT, and the corresponding mutant type (MT) vector pGL3-CLDN4-MT was constructed based on the mutated binding sequences. Well-constructed vectors were co-transfected with mimic control or miR-485-5p mimic in 293 T cells using the Lipofectamine™ 2000. After 48 h, the cells were collected and lysed, and the relative luciferase activity was evaluated on a Dual Luciferase Reporter Assay System (Promega). Three independent experiments were performed to collect the average value.

### 2.13. RNA immunoprecipitation (RIP) assay

An EZ-Magna-RIP Kit (Millipore) was used as per the kit's instructions. In brief, 48 h after transfection, cells were collected and treated with anti-Ago2 (Abcam) for RIP assay with IgG antibody served as a negative control. The immunoprecipitated RNA was determined using RT-qPCR.

### 2.14. Statistical analysis

SPSS 25.0 (IBM Corp. Armonk, NY, USA) was utilized for data analysis. Measurement data were exhibited as mean ± standard deviation (SD) from three independent experiments. Differenceswere compared by paired *t* test between two groups and one-way or two-way analysis of variance (ANOVA) followed by Tukey's multiple comparisontest among multiple groups. $p < 0.05$ was regarded to show significant difference.

## 3. Results

### 3.1. ELF3 is highly expressed in OC tissues and indicates poor prognosis in patients

As aforementioned, EFL3 has been reported to be linked to the initiation and development of gynecological tumors including cervical carcinoma and breast cancer, but its role in OC progression is not fully clear yet. We then searched the data available on the GEPIA System, which suggested a high expression profile of ELF3 in OC (Fig. 1A), and patients with lower ELF3 expression have a higher survival rate (Fig. 1B). In our experiments, also, we identified significantly increased positive ELF3 expression in the tumor tissues as compared to the adjacent normal ones from OC patients (Fig. 1C). In addition, the RT-qPCR results found an increase in ELF3

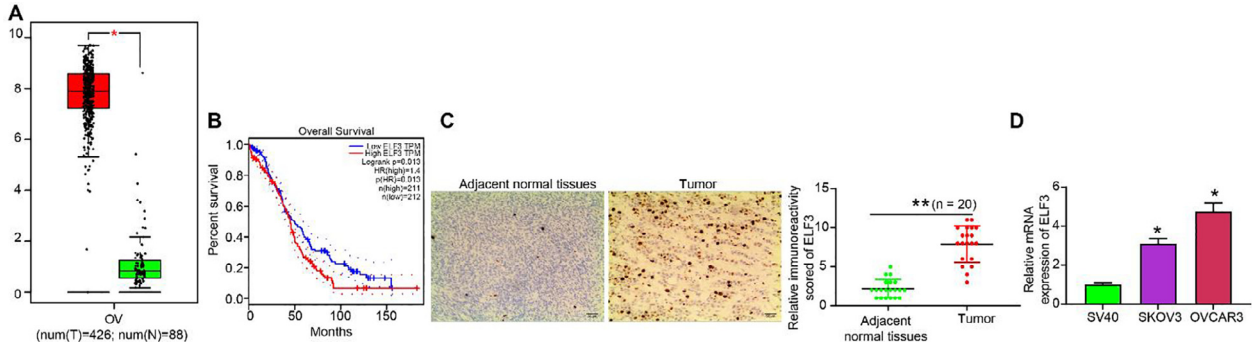


**Fig. 1.** ELF3 is highly expressed in OC tissues and associated with poor prognosis in patients. A, ELF3 expression profile in OC according to the data on the Bioinformation system GEPIA (http://gepia.cancer-pku.cn/); B, negative correlation between ELF3 expression and survival rate of OC patients suggested by GEPIA; C, ELF3 expression in OC tumor tissues and the paired normal tissues determined by immunohistochemical staining (paired *t* test, $^{**}p < 0.01$); D, ELF3 expression in OC cell lines (SKOV3 and OVCAR3) and immortalized human ovarian epithelial cells (SV40) measured by RT-qPCR. Data were exhibited as mean ± SD from three independent experiments.

level in OC cell lines (SKOV3 and OVCAR3) relative to the normal SV40 cells (Fig. 1D).

### 3.2. ELF3 inhibition reduces proliferation and triggers apoptosis of OC cell lines

To confirm the role of ELF3 in OC progression, artificial downregulation of ELF3 was introduced in cells through administration of sh-ELF3 1, 2, or 3#, after which the ELF3 expression was detected by RT-qPCR (Fig. 2A). Among the three shRNAs, sh-ELF3 1#, found with the best interfering efficacy, was used for the subsequent experiments (briefly defined as sh-ELF3 in the following text). OC cells with stable sh-ELF3 transfection were then collected for further use.

First, the MTT assay suggested that the viability of SKOV3 and OVCAR3 cells was decreased following ELF3 downregulation (Fig. 2B). A same trend was evidenced by the colony formation assay, sh-ELF3 transfection led to a significant decline in the number for formed cell colonies (Fig. 2C). Further, the ELISA results identified the protein level of pro-apoptotic factor Bax was increased while the level of the anti-apoptotic Bcl-2 was decreased upon ELF3 inhibition (Fig. 2D). More directly, the flow cytometry results revealed a notable increase in cell apoptosis rate following sh-ELF3 transfection (Fig. 2E). These findings collectively pointed out the suppressing role of ELF3 inhibition in OC cell growth.

### 3.3. ELF3 inhibition suppresses invasion and EMT of OC cells

The metastasis ability of OC cells after sh-ELF3 transfection was measured as well. The scratch test results showed that migration distance of sh-ELF3 was decreased after sh-ELF3 transfection (Fig. 3A). A similar trend was found by the Transwell assay which suggested the invasion ability of cells was reduced (Fig. 3B). In addition, the western blot analysis results suggested that the protein level of E-cadherin was increased while the protein level of vimentin was inhibited upon ELF3 inhibition (Fig. 3C).

### 3.4. ELF3 suppresses miR-485-5p transcription

ELF3 is a transcription factor that can mediate gene transcription. Here, we predicted on the bioinformatics system Jaspar (http://jaspar.genereg.net/) that ELF3 can bind to the promoter

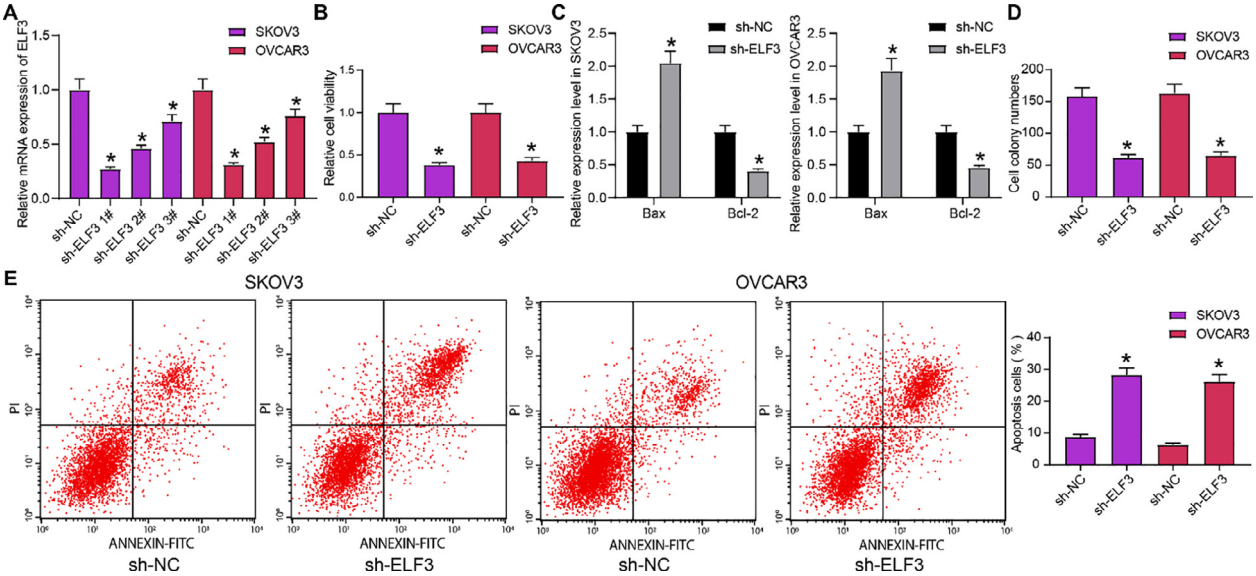


**Fig. 2.** ELF3 inhibition reduces proliferation and triggers apoptosis of OC cell lines. A, mRNA expression of ELF3 in cells after sh-ELF3 1, 2 or 3# transfection determined by RT-qPCR (one-way ANOVA, $^{*}p < 0.05$ compared to sh-NC transfection); B, viability of OC cell lines evaluated by the MTT assay (one-way ANOVA, $^{*}p < 0.05$); C, proliferation of OC cell lines determined by the colony formation assay (one-way ANOVA, $^{*}p < 0.05$); D, protein levels of apoptosis-related factors (Bax and Bcl-2) in OC cells measured by ELISA kits; E, apoptosis rate of OC cell lines detected by flow cytometry (one-way ANOVA, $^{*}p < 0.05$). Data were exhibited as mean ± SD from three independent experiments.

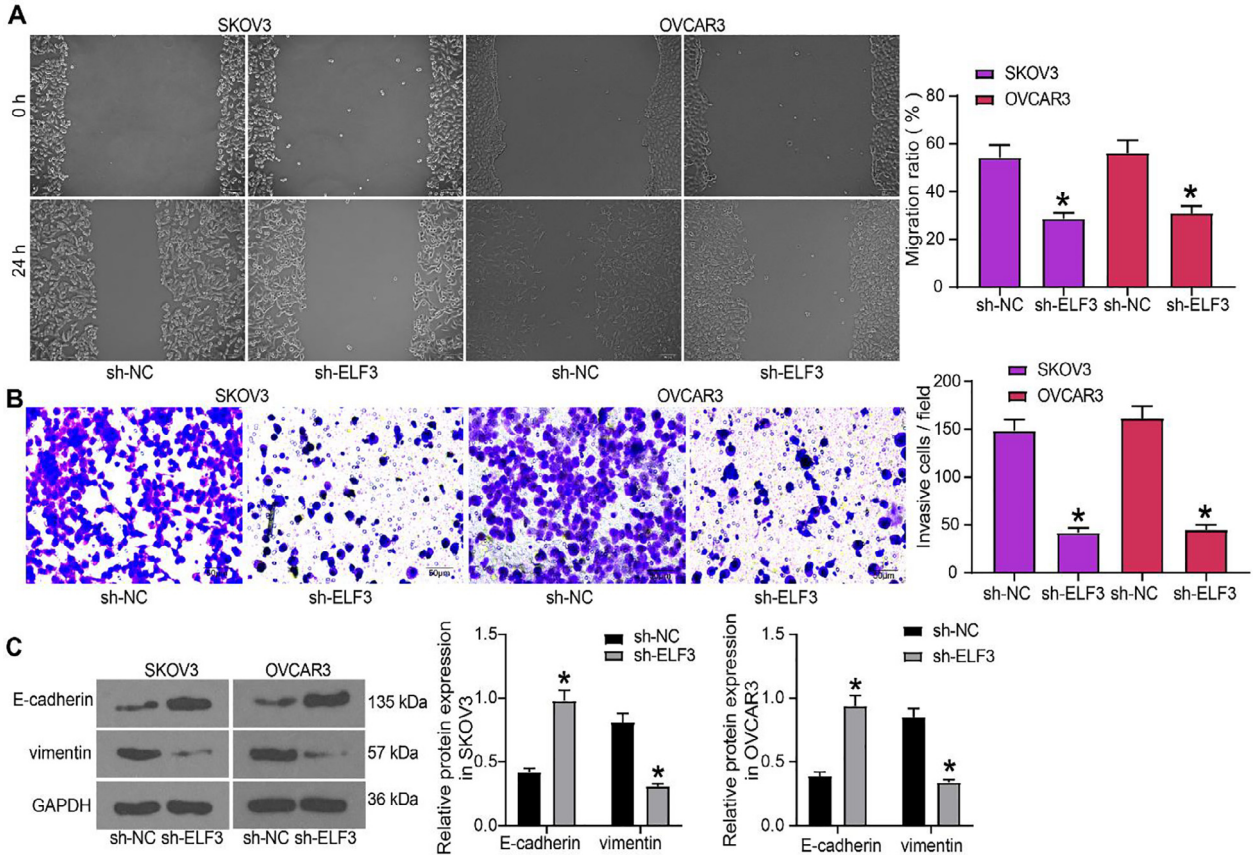


**Fig. 3.** ELF3 inhibition suppresses invasion and EMT of OC cells. A-B, migration (A) and invasion (B) abilities of OC cells detected by the scratch test and Transwell assay, respectively (one-way ANOVA, $^{*}p < 0.05$); C, protein levels of EMT-related biomarkers (E-cadherin and vimentin) detected by western blot analysis (two-way ANOVA, $^{*}p < 0.05$). Data were exhibited as mean ± SD from three independent experiments.

region of miR-485-5p (Fig. 4A). Since poor expression of miR-485-5p was suggested in OC cells and negatively related to chemoresistance, we speculated that downregulation of miR-485-5p is possibly accountable for the oncogenic role of ELF3. Thereafter, we determined miR-485-5p expression was lower in tumor tissues than that in adjacent normal tissues (Fig. 4B). Still, a decreased miR-485-5p expression profile was found in OC cell lines as compared to SV40 cells (Fig. 4C).

A

| Matrix ID | Name | Score | Relative score | Sequence ID | Start | End | Strand | Predicted sequence |
|---|---|---|---|---|---|---|---|---|
| MA0640.2 | ELF3 | 11.6364 | 0.879942475289 | hg38_knownGene_ENST00000385292.4 | 979 | 992 | + | aaggacttcctgga |
| MA0640.2 | ELF3 | 8.37035 | 0.818438327538 | hg38_knownGene_ENST00000385292.4 | 85 | 98 | - | acccacatcctcag |
| MA0640.2 | ELF3 | 8.24538 | 0.816048424366 | hg38_knownGene_ENST00000385292.4 | 1811 | 1824 | - | gggcactgccttct |
| MA0640.1 | ELF3 | 6.85591 | 0.806943589315 | hg38_knownGene_ENST00000385292.4 | 981 | 993 | - | gtccaggaagtcc |
| MA0640.2 | ELF3 | 7.71047 | 0.806011591216 | hg38_knownGene_ENST00000385292.4 | 1356 | 1369 | - | aaagtcttcctgga |

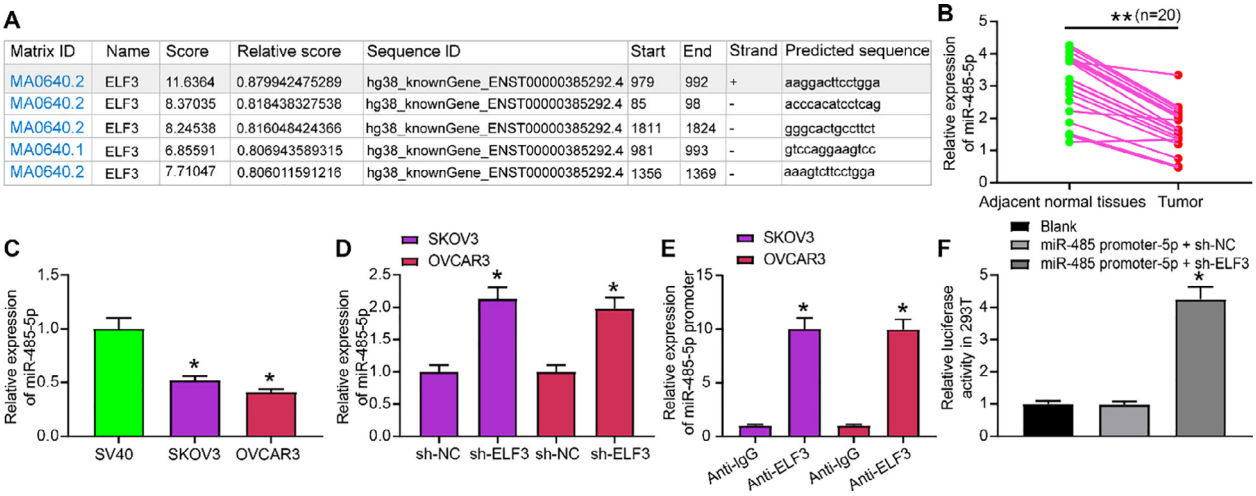


**Fig. 4.** ELF3 suppresses miR-485-5p transcription. A, binding sites between ELF3 and miR-485-5p predicted on Jaspar (http://jaspar.genereg.net/); B, miR-485-5p expression in OC tumor tissues and normal ones determined by RT-qPCR (paired *t* test, $^{**}p < 0.01$); C, miR-485-5p expression in OC cell lines and SV40 cells determined by RT-qPCR (one-way ANOVA, $^{*}p < 0.05$ compared to SV40 cells); D, miR-485-5p expression in OC cells after sh-ELF3 transfection measured by RT-qPCR (one-way ANOVA, $^{*}p < 0.05$); E, miR-485-5p promoter sequence enriched by anti-ELF3 or IgG antibody determined by ChIP assay and RT-qPCR (one-way ANOVA, $^{*}p < 0.05$); F, binding relationship between ELF3 and miR-485-5p validated through a luciferase assay (one-way ANOVA, $^{*}p < 0.05$, compared to miR-485-5p promoter + sh-NC). Data were exhibited as mean ± SD from three independent experiments.

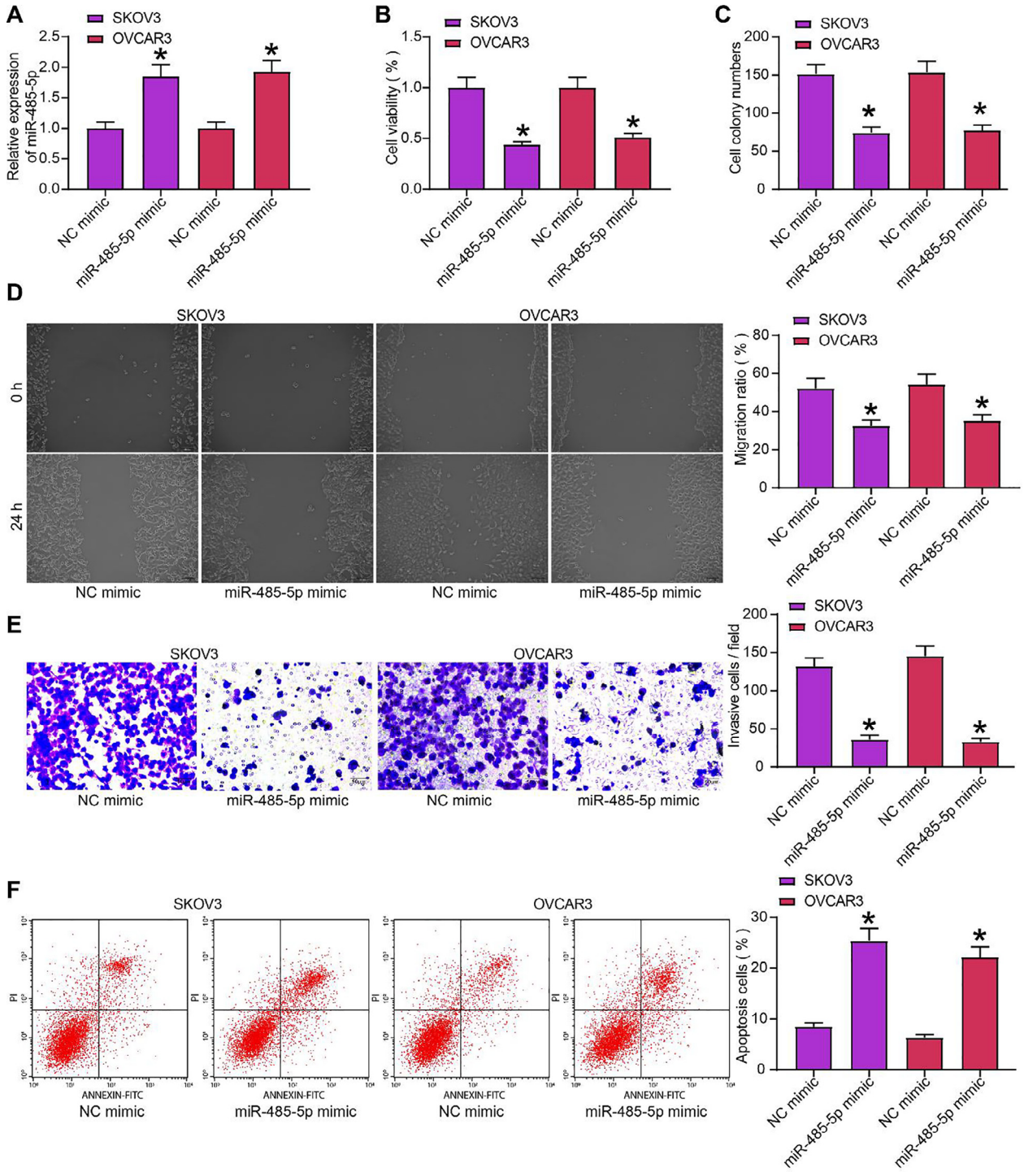


**Fig. 5.** Overexpression of miR-485-5p inhibits malignancy of OC cells. A, miR-485-5p expression in OC cell lines after miR-485-5p mimic transfection measured by RT-qPCR (one-way ANOVA, $^*p < 0.05$); B-C, viability (B) and proliferation (C) of OC cell lines determined by MTT and cell colony formation assays, respectively (one-way ANOVA, $^*p < 0.05$); D-E, migration (D) and invasion (E) abilities of OC cells measured by scratch test and Transwell assay, respectively (one-way ANOVA, $^*p < 0.05$); F, apoptosis of OC cells measured by flow cytometry (one-way ANOVA, $^*p < 0.05$). Data were exhibited as mean ± SD from three independent experiments.

In order to validate the binding relationship between ELF3 and miR-485-5p, RT-qPCR was performed to evaluate miR-485-5p expression in cells after sh-ELF3 transfection, which suggested that sh-ELF3 inhibited miR-485-5p expression in OC cells (Fig. 4D). The promoter sequence of miR-485-5p with highest score on the Jasper system was used for a ChIP assay. The results suggested that the anti-ELF3 enriched the promoter sequence of miR-485-5p as compared to the IgG antibody (Fig. 4E). In addition, a luciferase reporter containing the promoter sequence of miR-485-5p was further constructed, and it was found the luciferase activity of the reporter was increased by miR-485-5p (Fig. 4F). Collectively, these findings suggested that ELF3 can bind to the promoter of miR-485-5p and suppress miR-485-5p transcription.

### 3.5. Overexpression of miR-485-5p inhibits malignancy of OC cells

To validate the role of miR-485-5p in OC cell growth, artificial upregulation of miR-485-5p was introduced using miR-485-5p

mimic, and the transfection efficiency was identified by RT-qPCR (Fig. 5A). Then, the MTT assay suggested that overexpression of miR-485-5p inhibits viability of cells (Fig. 5B). Again, the number of formed cell colonies was decreased as well (Fig. 3C). The scratch test noted that the migration ability of cells was decreased (Fig. 5D), and the number of invaded cells, still, was reduced according to the Transwell assay (Fig. 5E). In terms of apoptosis, the flow cytometry results suggested an increase in cell apoptosis following miR-485-5p upregulation (Fig. 5F).

### 3.6. miR-485-5p targets CLDN4 to regulate the Wnt/β-catenin signaling

Data on Starbase predicted that miR-485-5p could bind to CLDN4 (Fig. 6A). CLDN4 was reported to be negatively linked to the overall survival of OC patients [15]. The data on GEPIA further suggested an abundance of CLDN4 in OC tissues (Fig. 6B). Then, our immunohistochemical staining results found CLDN4 was highly expressed in tumor tissues as compared to the paired normal ones from OC patients (Fig. 6C). A similar trend was found between OC and SV40 cells, where RT-qPCR suggested an increased mRNA expression of CLDN4 in SKOV3 and OVCAR3 cells (Fig. 6D).

To validate the binding relationship between miR-485-5p and CLDN4, a dual-luciferase reporter assay was performed, in which we found the luciferase activity in cells co-transfected with pGL3-CLDN4-WT and miR-485-5p mimic was decreased, while the activity in cells transfected with MT vector of mimic control showed no notable changes (Fig. 6E).

In addition, miR-485-5p mimic, miR-485-5p mimic + LV-CLDN4 and the corresponding controls were administrated in OC cells. After that, the RT-qPCR results found that the mRNA expression of CLDN4 was inhibited significantly by miR-485-5p mimic, while this inhibition was blocked by the further effect of LV-CLDN4 (Fig. 6G). It was noteworthy that the protein levels of Wnt1 and β-catenin were suppressed by miR-485-5p mimic and then recovered by LV-CLND4 (Fig. 6H). Namely, miR-485-5p was found to target CLDN4 to inactivate the Wnt/β-catenin pathway.

### 3.7. Upregulation of CLDN4 diminishes the suppressing role of ELF3 inhibition in OC progression

To further confirm the enrollment of CLDN4 following ELF3 mediation, OC cells were further transfected with sh-NC, sh-ELF3 + LV-NC or sh-ELF3 + LV-CLDN4. Then, it was found that CLDN4 expression was notable suppressed by sh-ELF3 and then recovered by LV-CLDN4 again (Fig. 7A). Based on the findings above that sh-ELF3 inhibits the malignant behaviors of OC cells, we further explored the role of the further administration of sh-ELF3.

Still, the MTT assay was performed and identified that LV-CLDN4 blocked the inhibiting roles of sh-ELF3 in OC cell viability (Fig. 7B), and the colony formation ability inhibited by sh-ELF3

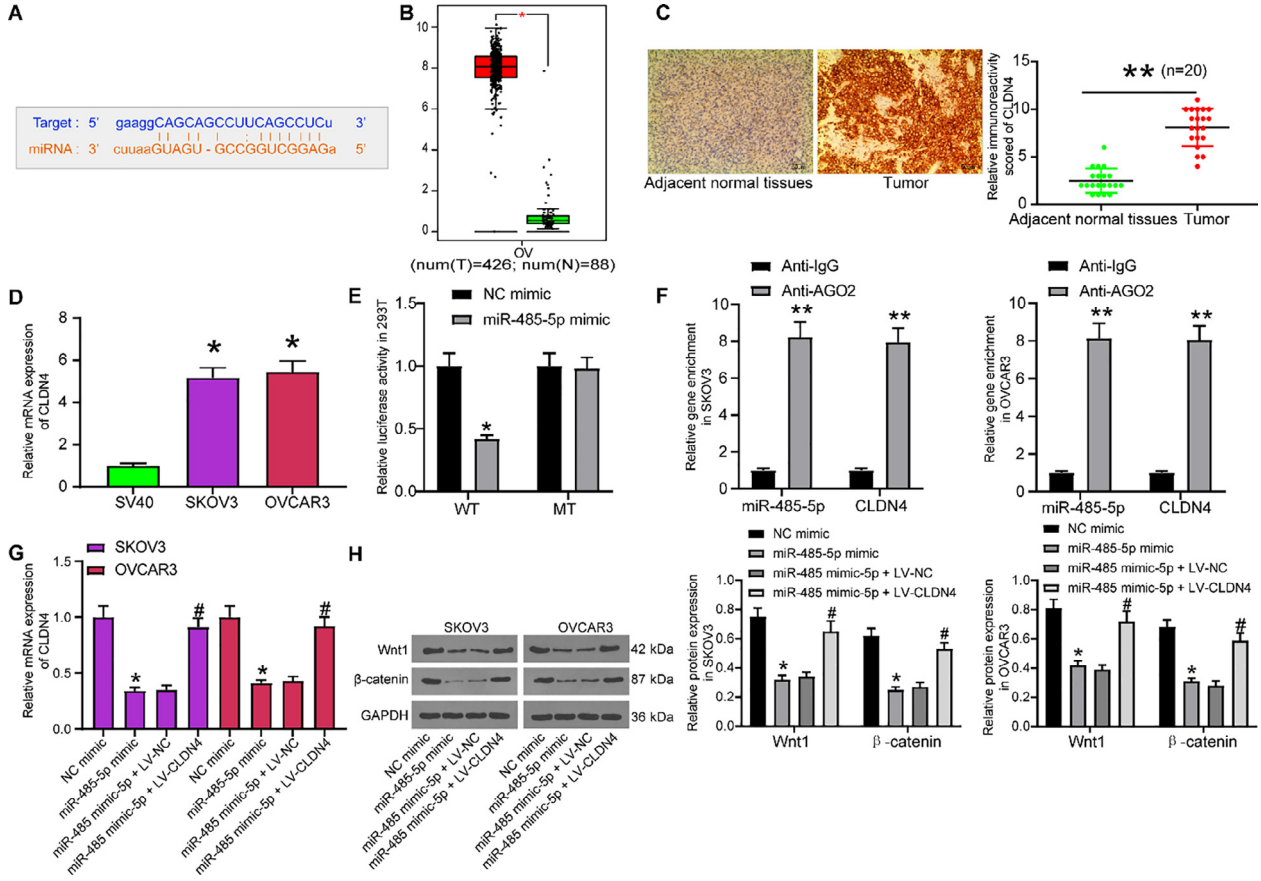


**Fig. 6.** miR-485-5p targets CLDN4 to regulate the Wnt/β-catenin signaling. A, binding site between miR-485-5p and CLDN4 predicted on Starbase (http://starbase.sysu.edu.cn/); B, miR-485-5p expression profile in OC predicted on GEPIA (http://gepia.cancer-pku.cn/); C, protein expression of CLDN4 in tumor tissues and the paired normal tissues determined by immunohistochemical staining (paired *t* test,$^{**}p < 0.01$); D, CLDN4 expression in OC cells and SV40 cells measured by RT-qPCR; E-F, binding relationship between miR-485-5p and CLDN4 validated through a dual luciferase reporter gene assay (E) and an RIP assay (F) (two-way ANOVA,$^{*}p < 0.05$); G, CLDN4 expression in OC cells after miR-485-5p mimic and LV-CLDN4 transfection determined by RT-qPCR (one-way ANOVA, $^{*}p < 0.05$ compared to NC mimic, $\#p < 0.05$ compared to miR-485-5p mimic + LV-NC); H, protein levels of Wnt1 and β-catenin in OC cell lines after miR-485-5p mimic and LV-CLDN4 transfection evaluated using western blot analysis (two-way ANOVA,$^{*}p < 0.05$ compared to NC mimic, $\#p < 0.05$ compared to miR-485-5p mimic + LV-NC). Data were exhibited as mean ± SD from three independent experiments.

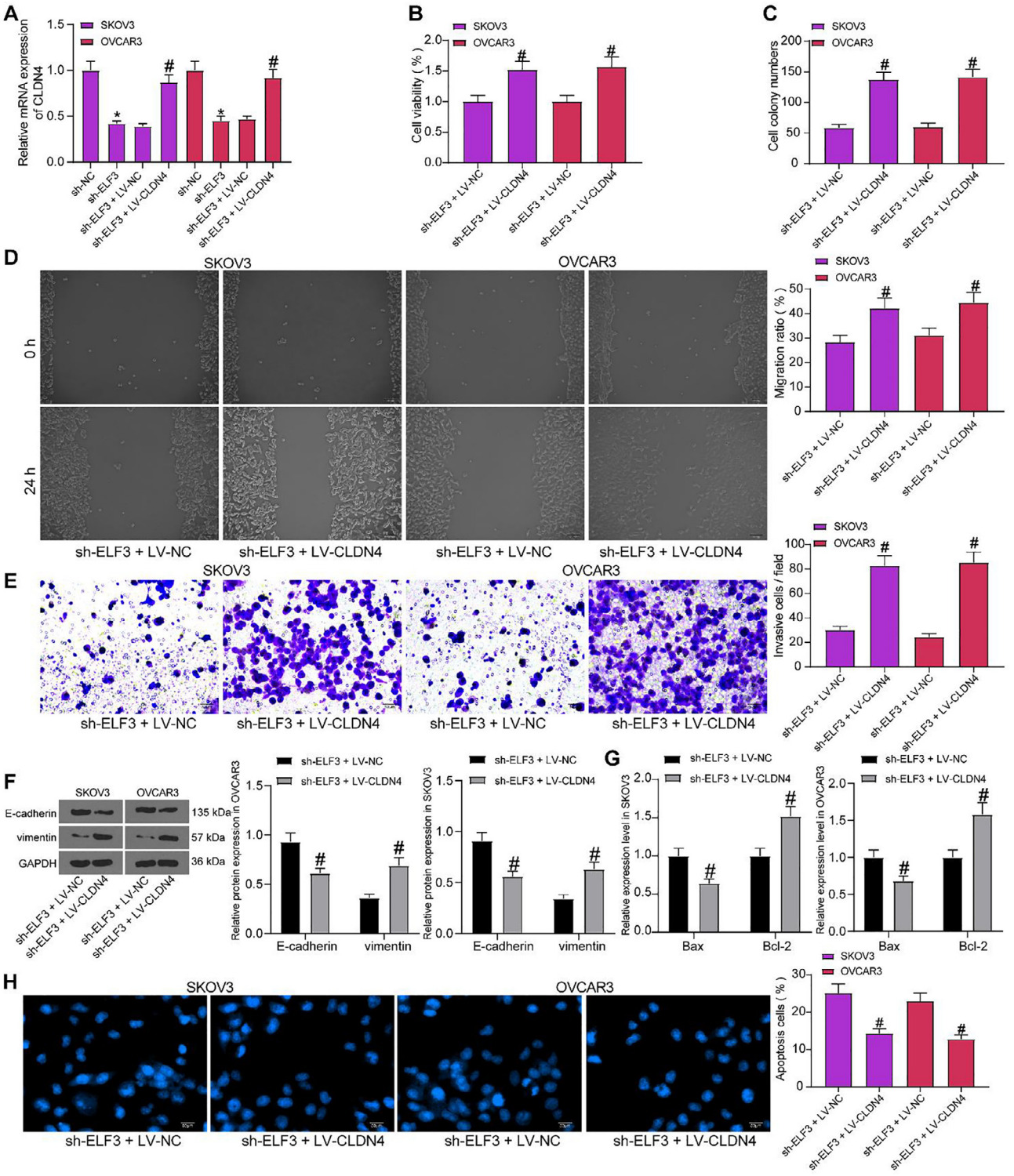


**Fig. 7.** Upregulation of CLDN4 diminishes the suppressing role of ELF3 inhibition in OC progression. A, mRNA expression of CLDN4 after sh-ELF3 or LV-CLDN4 transfection was determined by RT-qPCR (one-way ANOVA,*$p < 0.05$ compared to sh-NC, #$p < 0.05$ compared to sh-ELF3 + LV-NC); B-C, viability (B) and proliferation (C) of OC cell lines determined by MTT and cell colony formation assays, respectively (one-way ANOVA, *$p < 0.05$); D-E, migration (D) and invasion (E) abilities of OC cells measured by scratch test and Transwell assay, respectively (one-way ANOVA, *$p < 0.05$); F, protein levels of EMT-related biomarkers (E-cadherin and vimentin) detected by western blot analysis (two-way ANOVA, *$p < 0.05$); G, protein levels of apoptosis-related factors (Bax and Bcl-2) in OC cells measured by ELISA kits; H, apoptosis of OC cells measured by Hoechst 33,258 staining (one-way ANOVA, *$p < 0.05$). Data were exhibited as mean ± SD from three independent experiments.

was recovered following further upregulation of CLDN4 (Fig. 7C). Likewise, the inhibition on cell migration and invasion by sh-ELF3 was blocked upon CLDN4 overexpression (Fig. 7D-E). The western blot analysis results showed that the LV-CLDN4 inhibited E-cadherin expression while promoted vimentin expression in the presence of ELF3 silencing (Fig. 7F). The ELISA results confirmed a decline in Bax while an increase in Bcl-2 following further LV-CLDN4 expression (Fig. 7G). In addition, the Hoechst 33258

staining results showed that the apoptosis rate of OC cells was reduced by LV-CLDN4 (Fig. 7H).

## 4. Discussion

Though breast cancer is always taken into the primary consideration when it comes to the gynecologic malignancies because of the wide coverage, less is recognized that OC is the most fatal one (Stewart et al., 2019). The oncogenic roles of the ETS family of transcription factors have been concluded in solid tumors (Sizemore et al., 2017). Increased expression of the ETS transcription factors ELF3 and ETV3 through copy number gain at 1q21 and 1q32 has been noted to trigger tumorigenesis of breast cancer (Mesquita et al., 2013). In this research, we validated the tumor-promoting function of ELF3 in OC development, and a novel molecular mechanism involving miR-485-5p, CLDN4, and the Wnt/ signaling pathway.

ELF3 is abundantly existed in epithelial-rich tissues and is frequently correlated with epithelial-related cancers by influencing tumor proliferation, metastasis or differentiation (Zhao et al., 2018). Compared to the relatively abundant investigations regarding its correlation with breast cancer development (Kar et al., 2017; Zhang et al., 2020), the function of ELF3 in OC is less concerned. We first predicted a high expression profile of ELF3 in OC and its converse correlation with the survival of OC patients. To validate this, ELF3 expression in the collected OC tumor tissues and acquired cell lines was identified, with a finding that ELF3 is abundantly expressed both in cancer tissues and cells as relative to the normal ones. Further, artificial downregulation of ELF3 was introduced in OC cell lines, after which the viability and proliferation, migration and invasion, and EMT process were decreased, while the apoptosis rate of SKOV3 and OVCAR3 cells was increased (along with increased ratio of Bax to Bcl-2). Though defined as a tumor suppressor in cases, ELF3 was found to exert tumor promoting functions in epithelial-related cancers, such as in lung adenocarcinoma (Enfield et al., 2019; Ke et al., 2019). Likewise, downregulation of ELF3 by miR-320-3p was found to suppress invasion, migration and proliferation of lung cancer cells as well as the rumor growth rate in nude mice (Zhao et al., 2018). Similarly, a promoting role of ELF3 in EMT process was found in hepatocellular carcinoma, during which the transcriptional suppression in miR-141-3p and upregulation of ZEB1 were involved (Zheng et al., 2018).

As a transcription factor, ELF3 might fulfill its function in OC progression through modulating the transcription of the downstream transcripts, and then the promoter region of miR-485-5p was identified as the target of ELF3 through integrated bioinformatics prediction, ChIP and luciferase assays. miR-485-5p attracted our attention since it has been reported as a tumor suppressor in previous studies. It inhibited breast cancer progression and chemoresistance through targeting surviving (Wang et al., 2018) or MUC1 (Wang et al., 2020). Reduction in miR-485-5p expression in HPV-infected cervical cancer led to an increase in cell proliferation and invasion (Dai et al., 2020). As for in OC, miR-485-5p was found to be poorly expressed in tumors and associated with disease grade (Kim et al., 2010), and as aforementioned, to increase chemosensitivity of OC cells (Qiao et al., 2020). To further validate the miR-485-5p in the behaviors of OC cells and its association with ELF3, we found that miR-485-5p was suppressed by ELF3, while miR-485-5p mimic inhibited the malignant behaviors of OC cell lines. In addition, CLDN4 was identified as a target mRNA of miR-485-5p through online prediction, dual-luciferase and RIP assays. Importantly, the aforementioned tumor suppressing roles by ELF3 inhibition were blocked by the following artificial upregulation of CLDN4. This validated that miR-485-5p-mediated CLDN4 inhibition is at least partially implicated in the events following ELF3 inhibition. CLDN4 is a widely accepted oncogene from the Claudin tight-junction proteins and a promising target for anticancer therapy (Hashimi et al., 2013), whose inhibition leads to a diminished resistance to chemotherapies of cancer cells (Luo et al., 2020; Nishiguchi et al., 2019), and this is also applied in OC cells (Gao et al., 2011; Yoshida et al., 2011). This further promoted that ELF3 inhibition may lead to CLDN4 silencing and improve the sensitivity of chemotherapies.

The Wnt/β-catenin axis modulates cell proliferation, survival, polarity, and stem cell fate in tissue homeostasis, while its aberrant activation affects multiple key aspects of cancer progression from metastasis to chemoresistance, including OC (Nguyen et al., 2019). Specifically, miR-485-5p inhibition was found toactivate the Wnt/β-catenin signaling and to trigger progression of hepatocellular carcinoma (Wang et al., 2018). In this research, miR-485-5p mimic was found to inactivate the Wnt/β-catenin pathway, but this inactivation was blocked by the further administration of LV-CLDN4, indicating this pathway is partially responsible for the oncogenic role of CLDN4.

## 5. Conclusions

ELF3 suppresses miR-485-5p transcription to enhance CLDN4 expression, leading to Wnt/β-catenin activation and promoting OC cell growth and metastasis. However, the main limitation is that *in vivo* experiments were not involved in the current work. We would like to validate these findings in animal models in our further experiments, and, if possible, we would also perform a follow-up study to analyze the correlations of these factors with the clinical presentation and prognosis of OC patients. We hope these findings may provide new thoughts into OC treatment.

## Funding

This work was supported by Lianyungang Health and Family Planning Science and Technology Project (201814).

## 7. Ethics statement

This study was launched with the approval of the Ethics Committee of our hospital and performed in compliance with the Declaration of Helsinki. Signed informed consent was received from each eligible participant.

## Declaration of Competing Interest

The authors declare that they have no known competing financial interests or personal relationships that could have appeared to influence the work reported in this paper.

## References

Alimujiang, A., Khoja, L., Wiensch, A., Pike, M.C., Webb, P.M., Chenevix-Trench, G., Chase, A., Richardson, J., Pearce, C.L., 2019. "I am not a statistic" ovarian cancer survivors' views of factors that influenced their long-term survival. Gynecol. Oncol. 155 (3), 461–467.

Cress, R.D., Chen, Y.S., Morris, C.R., Petersen, M., Leiserowitz, G.S., 2015. Characteristics of long-term survivors of epithelial ovarian cancer. Obstet. Gynecol. 126 (3), 491.

Dai, Y., Xie, F., Chen, Y., 2020. Reduced levels of miR-485-5p in HPV-infected cervical cancer promote cell proliferation and enhance invasion ability. FEBS Open Bio. 10 (7), 1348.

de la Fuente, L.M., Malander, S., Hartman, L., Jönsson, J.M., Ebbesson, A., Nilbert, M., Måsbäck, A., Hedenfalk, I., 2018. Claudin-4 expression is associated with survival in ovarian cancer but not Pt K witk with chemotherapy response. Int. Gynecol. Pathol. 37 (2), 101.

Enfield, K.S., Marshall, E.A., Anderson, C., Ng, K.W., Rahmati, S., Xu, Z., Fuller, M., Milne, K., Lu, D., Shi, R., Rowbotham, D.A., 2019. Epithelial tumor suppressor

ELF3 is a lineage-specific amplified oncogene in lung adenocarcinoma. Nat. Commun. 10 (1), 1–13.
Gajulapalli, V.N.R., Samanthapudi, V.S.K., Pulaganti, M., Khumukcham, S.S., Malisetty, V.L., Guruprasad, L., Chitta, S.K., Manavathi, B., 2016. A transcriptional repressive role for epithelial-specific ETS factor ELF3 on oestrogen receptor alpha in breast cancer cells. Biochem. J. 473 (8), 1047–1061.
Gao, Z., Xu, X., McClane, B., Zeng, Q., Litkouhi, B., Welch, W.R., Berkowitz, R.S., Mok, S.C., Garner, E.I., 2011. C terminus of *Clostridium perfringens* enterotoxin downregulates CLDN4 and sensitizes ovarian cancer cells to Taxol and Carboplatin. Clin. Cancer Res. 17 (5), 1065–1074.
Gondkar, K., Patel, K., Krishnappa, S., Patil, A., Nair, B., Sundaram, G.M., Zea, T.T., Kumar, P., 2019. E74 like ETS transcription factor 3 (ELF3) is a negative regulator of epithelial-mesenchymal transition in bladder carcinoma. Cancer Biomark. 25 (2), 223–232.
Harrandah, A.M., Mora, R.A., Chan, E.K., 2018. Emerging microRNAs in cancer diagnosis, progression, and immune surveillance. Can. Res., 126–132
Hashimi, S.M., Yu, S., Alqurashi, N., Ipe, D.S., Wei, M.Q., 2013. Immunotoxin-mediated targeting of claudin-4 inhibits the proliferation of cancer cells. Int. J. Oncol. 42 (6), 1911–1918.
Honda, H., Pazin, M.J., Ji, H., Wernyj, R.P., Morin, P.J., 2006. Crucial roles of Sp1 and epigenetic modifications in the regulation of the CLDN4 promoter in ovarian cancer cells. J. Biol. Chem. 281 (30), 21433–21444.
Kar, A., Liu, B., Gutierrez-Hartmann, A., 2017. ESE-1 knockdown attenuates growth in trastuzumab-resistant HER2+ breast cancer cells. Anticancer Res. 37 (12), 6583–6591.
Ke, Z., Xie, F., Zheng, C., Chen, D., 2019. CircHIPK3 promotes proliferation and invasion in nasopharyngeal carcinoma by abrogating miR-4288-induced ELF3 inhibition. J. Cellular Physiol. 234 (2), 1699–1706.
Kim, T.H., Kim, Y.K., Kwon, Y., Heo, J.H., Kang, H., Kim, G., An, H.J., 2010. Deregulation of miR-519a, 153, and 485–5p and its clinicopathological relevance in ovarian epithelial tumours. Histopathology 57 (5), 734–743.
Lheureux, S., Braunstein, M., Oza, A.M., 2019. Epithelial ovarian cancer: evolution of management in the era of precision medicine. CA Cancer J. Clin. 69 (4), 280–304.
Luo, Y., Kishi, S., Sasaki, T., Ohmori, H., Fujiwara-Tani, R., Mori, S., Goto, K., Nishiguchi, Y., Mori, T., Kawahara, I., Kondoh, M., 2020. Targeting claudin-4 enhances chemosensitivity in breast cancer. Cancer Sci. 111 (5), 1840.
Mesquita, B., Lopes, P., Rodrigues, A., Pereira, D., Afonso, M., Leal, C., Henrique, R., Lind, G.E., Jerónimo, C., Lothe, R.A., Teixeira, M.R., 2013. Frequent copy number gains at 1q21 and 1q32 are associated with overexpression of the ETS transcription factors ETV3 and ELF3 in breast cancer irrespective of molecular subtypes. Brest Cancer Res. Treat. 138 (1), 37–45.
Nguyen, V.H.L., Hough, R., Bernaudo, S., Peng, C., 2019. Wnt/β-catenin signalling in ovarian cancer: Insights into its hyperactivation and function in tumorigenesis. J. Ovarian Res. 12 (1), 1–17.
Nishiguchi, Y., Fujiwara-Tani, R., Sasaki, T., Luo, Y., Ohmori, H., Kishi, S., Mori, S., Goto, K., Yasui, W., Sho, M., Kuniyasu, H., 2019. Targeting claudin-4 enhances CDDP-chemosensitivity in gastric cancer. Oncotarget 10 (22), 2189.
Ojesina, A.I., Lichtenstein, L., Freeman, S.S., Pedamallu, C.S., Imaz-Rosshandler, I., Pugh, T.J., Cherniack, A.D., Ambrogio, L., Cibulskis, K., Bertelsen, B., Romero-Cordoba, S., 2014. Landscape of genomic alterations in cervical carcinomas. Nature 506 (7488), 371–375.
Qiao, H.F., Liu, Y.L., You, J., Zheng, Y.L., Chen, L.P., Lu, X.Y., Du, L., Shan, F., Liu, M.H., 2020. G-5555 synergized miR-485-5p to alleviate cisplatin resistance in ovarian cancer cells via Pi3k/Akt signaling pathway. J. Reproduct. Immunol. 140, 103129.
Sizemore, G.M., Pitarresi, J.R., Balakrishnan, S., Ostrowski, M.C., 2017. The ETS family of oncogenic transcription factors in solid tumours. Nat. Rev. Cancer. 17 (6), 337.
Stewart, C., Ralyea, C., Lockwood, S., 2019. April. Ovarian cancer: an integrated review. Semin. Oncol. Nurs. 35 (2), 151–156.
Wang, J.L., Chen, Z.F., Chen, H.M., Wang, M.Y., Kong, X., Wang, Y.C., Sun, T.T., Hong, J., Zou, W., Xu, J., Fang, J.Y., 2014. Elf3 drives β-catenin transactivation and associates with poor prognosis in colorectal cancer. Cell Death Dis. 5 (5).
Wang, M., Cai, W.R., Meng, R., Chi, J.R., Li, Y.R., Chen, A.X., Yu, Y., Cao, X.C., 2018a. miR-485-5p suppresses breast cancer progression and chemosensitivity by targeting survivin. Biochem. Biophy. Res. Commun. 501 (1), 48–54.
Wang, X., Zhou, X., Zeng, F., Wu, X., Li, H., 2020. miR-485-5p inhibits the progression of breast cancer cells by negatively regulating MUC1. Breast Can. 27 (4), 765–775.
Wang, Y., Sun, L., Wang, L., Liu, Z., Li, Q., Yao, B., Wang, C., Chen, T., Tu, K., Liu, Q., 2018b. Long non-coding RNA DSCR8 acts as a molecular sponge for miR-485-5p to activate Wnt/β-catenin signal pathway in hepatocellular carcinoma. Cell Death Dis. 9 (9), 1–13.
Yoshida, H., Sumi, T., Zhi, X., Yasui, T., Honda, K.I., Ishiko, O., 2011. Claudin-4: a potential therapeutic target in chemotherapy-resistant ovarian cancer. Anticancer Res. 31 (4), 1271–1277.
Zahedi, P., De Souza, R., Huynh, L., Piquette-Miller, M., Allen, C., 2011. Combination drug delivery strategy for the treatment of multidrug resistant ovarian cancer. Mol. Pharmaceut. 8 (1), 260–269.
Zhang, Z., Zhang, J., Li, J., Geng, H., Zhou, B., Zhang, B., Chen, H., 2020. miR–320/ELF3 axis inhibits the progression of breast cancer via the PI3K/AKT pathway. Oncol. Lett. 19 (4), 3239–3248.
Zhao, W., Sun, Q., Yu, Z., Mao, S., Jin, Y., Li, J., Jiang, Z., Zhang, Y., Chen, M., Chen, P., Chen, D., 2018. MiR-320a-3p/ELF3 axis regulates cell metastasis and invasion in non-small cell lung cancer via PI3K/Akt pathway. Gene 670, 31–37.
Zheng, L., Xu, M., Xu, J., Wu, K., Fang, Q., Liang, Y., Zhou, S., Cen, D., Ji, L., Han, W., Cai, X., 2018. ELF3 promotes epithelial–mesenchymal transition by protecting ZEB1 from miR-141-3p-mediated silencing in hepatocellular carcinoma. Cell Death Dis. 9 (3), 1–14.